

# Logic Synthesis for Switching Lattices

Mustafa Altun and Marc D. Riedel

**Abstract**—This paper studies the implementation of Boolean functions by lattices of four-terminal switches. Each switch is controlled by a Boolean literal. If the literal takes the value 1, the corresponding switch is connected to its four neighbours; else it is not connected. A Boolean function is implemented in terms of connectivity across the lattice: it evaluates to 1 iff there exists a connected path between two opposing edges of the lattice. The paper addresses the following synthesis problem: how should one assign literals to switches in a lattice in order to implement a given target Boolean function? The goal is to minimize the lattice size, measured in terms of the number of switches. An efficient algorithm for this task is presented – one that does not exhaustively enumerate paths but rather exploits the concept of Boolean function *duality*. The algorithm produces lattices with a size that grows linearly with the number of products of the target Boolean function in ISOP form. It runs in time that grows polynomially. Synthesis trials are performed on standard benchmark circuits. The synthesis results are compared to a lower-bound calculation on the lattice size.

**Index Terms**—Boolean Functions, Switching Circuits, Lattices, Nanowire Crossbar Arrays



## 1 INTRODUCTION

In his seminal Master’s Thesis, Claude Shannon made the connection between Boolean algebra and switching circuits [2]. He considered two-terminal switches corresponding to electromagnetic relays. An example of a two-terminal switch is shown in the top part of Figure 1. The switch is either ON (closed) or OFF (open). A Boolean function can be implemented in terms of connectivity across a network of switches, often arranged in a series/parallel configuration. An example is shown in the bottom part of Figure 1. Each switch is controlled by a Boolean literal. If the literal is 1 (0) then the corresponding switch is ON (OFF). The Boolean function for the network evaluates to 1 if there is a closed path between the left and right nodes. It can be computed by taking the sum (OR) of the product (AND) of literals along each path. These products are  $x_1x_2x_3$ ,  $x_5x_1x_2x_6$ ,  $x_5x_4x_2x_3$ , and  $x_5x_4x_6$ .

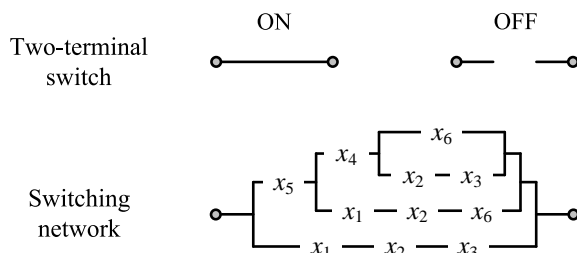


Fig. 1: Two-terminal switching network implementing the Boolean function  $x_1x_2x_3 + x_1x_2x_5x_6 + x_2x_3x_4x_5 + x_4x_5x_6$ .

In this paper, we develop a method for synthesizing Boolean functions with networks of four-terminal switches. An example is shown in the top part of Figure 2. The four terminals of the switch are all either

mutually connected (ON) or disconnected (OFF). We consider networks of four-terminal switches arranged in rectangular *lattices*. An example is shown in the bottom part of Figure 2. Again, each switch is controlled by a Boolean literal. If the literal takes the value 1 (0) then corresponding switch is ON (OFF). The Boolean function for the lattice evaluates to 1 iff there is a closed path between the top and bottom edges of the lattice. Again, the function is computed by taking the sum of the products of the literals along each path. These products are  $x_1x_2x_3$ ,  $x_1x_2x_5x_6$ ,  $x_4x_5x_2x_3$ , and  $x_4x_5x_6$  – the same as those in Figure 1. We conclude that this lattice of four-terminal switches implements the same Boolean function as the network of two-terminal switches in Figure 1.

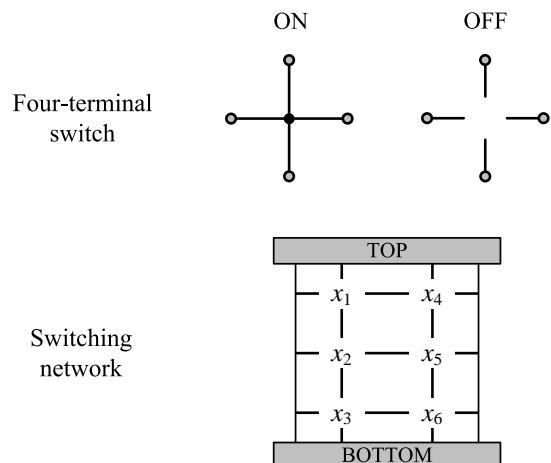


Fig. 2: Four-terminal switching network implementing the Boolean function  $x_1x_2x_3 + x_1x_2x_5x_6 + x_2x_3x_4x_5 + x_4x_5x_6$ .

Throughout the paper we will use a “checkerboard” representation for lattices where black and white sites represent ON and OFF switches, respectively, as illustrated in Figure 3. We will discuss the Boolean functions implemented in terms of connectivity between the top

- This work is supported by an NSF CAREER award #0845650.
- E-mail: {altu0006, mriedel}@umn.edu
- A preliminary version of this paper appeared in [1].

and bottom edges as well as connectivity between the left and right edges. (We will refer to these edges as “plates”).

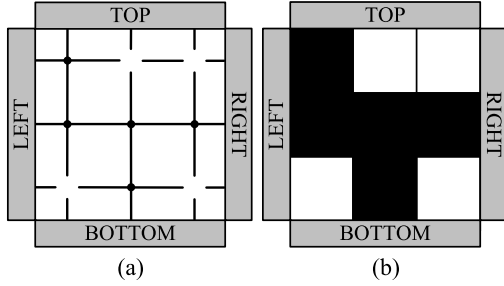


Fig. 3: A  $3 \times 3$  four-terminal switch network and its lattice form.

This paper addresses the following synthesis problem: how should we assign literals to switches in a lattice in order to implement a given target Boolean function? Suppose that we are asked to implement the function  $f(x_1, x_2, x_3, x_4) = x_1x_2x_3 + x_1x_4$ . We might consider the lattice in Figure 4(a). The product of the literals in the first column is  $x_1x_2x_3$ ; the product of the literals in the second column is  $x_1x_4$ . We might also consider the lattice in Figure 4(b). The products for its columns are the same as those for (a). In fact, the two lattices implement two different functions, only one of which is the intended target function. To see why this is so, note that we must consider all possible paths, including those shown by the red and blue lines. In (a) the product  $x_1x_2$  corresponding to the path shown by the red line covers the product  $x_1x_2x_3$  so the function is  $f_a = x_1x_2 + x_1x_4$ . In (b) the products  $x_1x_2x_4$  and  $x_1x_2x_3x_4$  corresponding to the paths shown by the red and blue lines are redundant, covered by column paths, so the function is  $f_b = x_1x_2x_3 + x_1x_4$ .

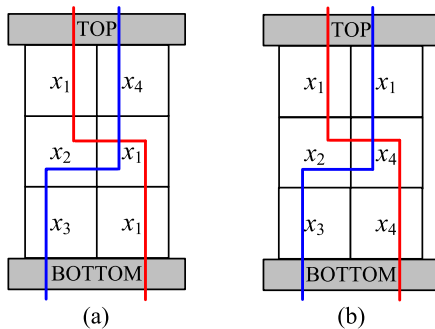


Fig. 4: Two  $3 \times 2$  lattices implementing different Boolean functions.

In this example, the target function is implemented by a  $3 \times 2$  lattice with four paths. If we were given a target function with more products, a larger lattice would likely be needed to implement it; accordingly, we would need to enumerate more paths. Here the problem is that number of paths grows exponentially with the lattice size. Any synthesis method that enumerates paths quickly becomes intractable. We present an efficient algorithm

for this task – one that does not exhaustively enumerate paths but rather exploits the concept of Boolean function *duality* [3], [4]. Our synthesis algorithm produces lattices with a size that grows linearly with the number of products of the target Boolean function. It runs in time that grows polynomially.

The paper is organized as follows. In Section 2, we discuss potential technologies that fit our model of regular lattices of four-terminal switches. In Section 3, we present our general synthesis method that implements any target function with a lattice of four-terminal switches. In Section 4, we discuss the implementation of a specific function, the *parity function*. In Section 5, we derive a lower bound on the size of a lattice required to implement a Boolean function. In Section 6, we evaluate our general synthesis method on standard benchmark circuits. In Section 7, we discuss extensions and future directions for this research.

## 1.1 Definitions

**Definition 1** Consider  $k$  independent Boolean variables,  $x_1, x_2, \dots, x_k$ . **Boolean literals** are Boolean variables and their complements, i.e.,  $x_1, \bar{x}_1, x_2, \bar{x}_2, \dots, x_k, \bar{x}_k$ .

**Definition 2** A **product (P)** is an AND of literals, e.g.,  $P = x_1\bar{x}_3x_4$ . A **set of a product (SP)** is a set containing all the product’s literals, e.g., if  $P = x_1\bar{x}_3x_4$  then  $SP = \{x_1, \bar{x}_3, x_4\}$ . A **sum-of-products (SOP)** expression is an OR of products.

**Definition 3** A **prime implicant (PI)** of a Boolean function  $f$  is a product that implies  $f$  such that removing any literal from the product results in a new product that does not imply  $f$ .

**Definition 4** An **irredundant sum-of-products (ISOP)** expression is an SOP expression, where each product is a PI and no PI can be deleted without changing the Boolean function  $f$  represented by the expression.

**Definition 5**  $f$  and  $g$  are **dual Boolean functions** iff

$$f(x_1, x_2, \dots, x_k) = \bar{g}(\bar{x}_1, \bar{x}_2, \dots, \bar{x}_k).$$

Given an expression for a Boolean function in terms of AND, OR, NOT, 0, and 1, its dual can also be obtained by interchanging the AND and OR operations as well as interchanging the constants 0 and 1. For example, if  $f(x_1, x_2, x_3) = x_1x_2 + \bar{x}_1x_3$  then  $f^D(x_1, x_2, x_3) = (x_1 + x_2)(\bar{x}_1 + x_3)$ . A trivial example is that for  $f = 1$ , the dual is  $f^D = 0$ .

**Definition 6** A **parity function** is a Boolean function that evaluates to 1 iff the number of variables assigned to 1 is an odd number. The parity function  $f$  of  $k$  variables can be computed by the exclusive-OR (XOR) of the variables:  $f = x_1 \oplus x_2 \oplus \dots \oplus x_k$ .

## 2 APPLICABLE TECHNOLOGIES

The concept of regular two-dimensional arrays of four-terminal switches is not new; it dates back to a seminal paper by Akers in 1972 [5]. With the advent of a variety of types of emerging nanoscale technologies, the model has found renewed interest [6], [7]. Unlike conventional CMOS that can be patterned in complex ways with lithography, self-assembled nanoscale systems generally consist of regular structures. Logical functions are achieved with crossbar-type switches [8], [9]. Although conceptually general, our model corresponds to exactly this type of switch in a variety of emerging technologies.

A schematic for the realization of our model is shown in Figure 5. Each site of the lattice is a four-terminal switch, controlled by an input voltage. When a high (logic 1) or low (logic 0) voltage is applied, the switch is ON or OFF, respectively. The output of the circuit depends upon the top-to-bottom connectivity across the lattice. If the top and bottom plates are connected, then the lattice allows signals to flow; accordingly, the output is logic 1. Otherwise the output is logic 0. The output can be sensed with a resistor connected to the bottom plate while a high voltage applied to the top plate. Below, we discuss two potential technologies that fit our model.

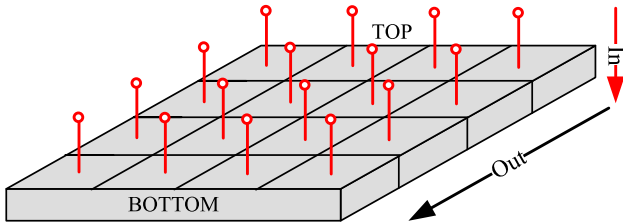


Fig. 5: 3D realization of our circuit model with the inputs and the output.

In their seminal work, Yi Cui and Charles Lieber investigated crossbar structures for different types of nanowires including  $n$ -type and  $p$ -type nanowires [10]. They achieved the different types of junctions by crossing different types of nanowires.

By crossing an  $n$ -type nanowire and a  $p$ -type nanowire, they achieved a diode-like junction. By crossing two  $n$ -types or two  $p$ -types, they achieved a resistor-like junction (with a very low resistance value). They showed that the connectivity of nanowires can be controlled by an insulated input voltage  $V$ -in. A high  $V$ -in makes the  $p$ -type nanowires conductive and the  $n$ -type nanowires resistive; a low  $V$ -in makes the  $p$ -type nanowires resistive and the  $n$ -type nanowires conductive. So they showed that, based on a controlling voltage, nanowires can behave either like short circuits or like open circuits.

A four-terminal switch can be implemented with the techniques of Cui and Lieber, as illustrated in Figure 6. The switch has crossed  $p$ -type nanowires. When a high  $V$ -in is applied, the nanowires behave like short circuits.

A resistor-like junction is formed, with low resistance. Thus, all four terminals are connected; the switch is ON. When a low  $V$ -in is applied, the nanowires behave like open circuits: all four terminals are disconnected; the switch is OFF. The result is a four-terminal switch that corresponds to our model.

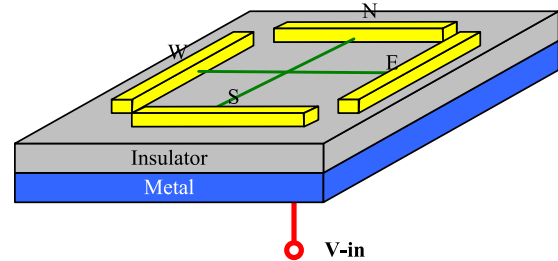


Fig. 6: Nanowire four-terminal switch.

Nanowire switches, of course, are assembled in large arrays. Indeed, the impetus for nanowire-based technology is the potential density, scalability and manufacturability [11]–[13]. Consider a  $p$ -type nanowire array, where each crosspoint is controlled by an input voltage. From the discussion above, we know that each such crosspoint behaves like a four-terminal switch. Accordingly, the nanowire crossbar array can be modeled as a lattice of four-terminal switches as illustrated in Figure 7. Here the black and white sites represent crosspoints that are ON and OFF, respectively.

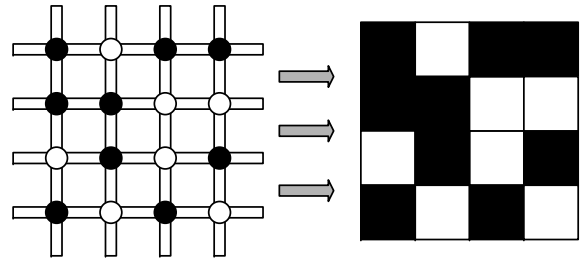


Fig. 7: Nanowire crossbar array with random connections and its lattice representation.

Nanowire crossbar arrays may offer substantial advantages over conventional CMOS when used to implement programmable architectures. Conventional implementations typically employ SRAMs for programming crosspoints. However, for nanoscale technologies, relative to the size of the switches, SRAMs would be prohibitively costly. A variety of techniques have been suggested for fabricating programmable nanowire crosspoints based on bistable switches that form memory cores [13], [14]. Also, molecular switches and solid-electrolyte nanoswitches could be used to form programmable crosspoints [15].

Other novel and emerging technologies fit our model of four-terminal switches. For instance, researchers are investigating *spin waves* [16]. Unlike conventional circuitry such as CMOS that transmits signals electrically, spin-wave technology transmits signals as propagating

disturbances in the ordering of magnetic materials. Potentially, spin-wave based logic circuits could compute with significantly less power than conventional CMOS circuitry.

Spin wave switches are four-terminal devices, as illustrated in Figure 8. They have two states ON and OFF, controlled by an input voltage  $V_{in}$ . In the ON state, the switch transmits all spin waves; all four terminals are connected. In the OFF state, the switch reflects any incoming spin waves; all four terminals are disconnected. Spin-wave switches, like nanowire switches, are also configured in crossbar networks [17].

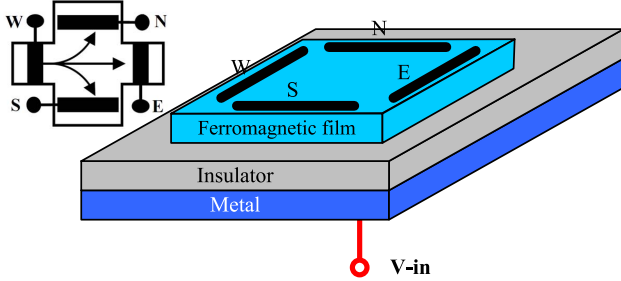


Fig. 8: Spin-wave switch.

### 3 SYNTHESIS METHOD

In our synthesis method, a Boolean function is implemented by a lattice according to the connectivity between the top and bottom plates. In order to elucidate our method, we will also discuss connectivity between the left and right plates. Call the Boolean functions corresponding to the top-to-bottom and left-to-right plate connectivities  $f_L$  and  $g_L$ , respectively. As shown in Figure 9, each Boolean function evaluates to 1 if there exists a path between corresponding plates, and evaluates to 0 otherwise. Thus,  $f_L$  can be computed as the OR of all top-to-bottom paths, and  $g_L$  as the OR of all left-to-right paths. Since each path corresponds to the AND of inputs, the paths taken together correspond to the OR of these AND terms, so implement sum-of-products expressions.

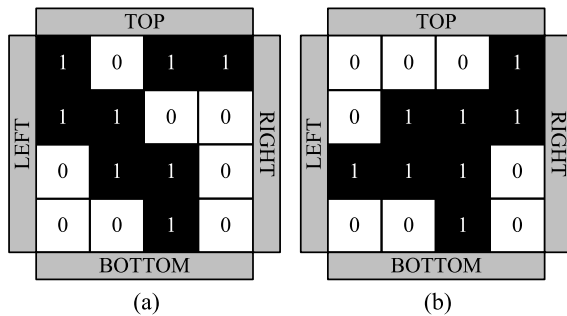


Fig. 9: Relationship between Boolean functionality and paths. (a):  $f_L = 1$  and  $g_L = 0$ . (b):  $f_L = 1$  and  $g_L = 1$ .

**Example 1** Consider the lattice shown in Figure 10. It consists of six switches. Consider the three top-to-bottom paths

$x_1x_4$ ,  $x_2x_5$ , and  $x_3x_6$ . Consider the four left-to-right paths  $x_1x_2x_3$ ,  $x_1x_2x_5x_6$ ,  $x_4x_5x_2x_3$ , and  $x_4x_5x_6$ . While there are other possible paths, such as the one shown by the dashed line, all such paths are covered by the paths listed above. For instance, the path  $x_1x_2x_5$  shown by the dashed line is covered by the path  $x_2x_5$  shown by the solid line, and so is redundant. We conclude that the top-to-bottom function is the OR of the three products above,  $f_L = x_1x_4 + x_2x_5 + x_3x_6$ , and the left-to-right function is the OR of the four products above,  $g_L = x_1x_2x_3 + x_1x_2x_5x_6 + x_2x_3x_4x_5 + x_4x_5x_6$ .

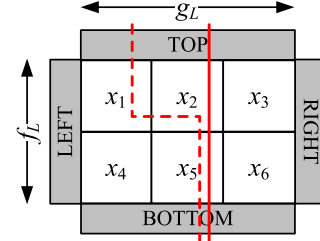


Fig. 10: A  $2 \times 3$  lattice with assigned literals.

We address the following logic synthesis problem: given a target Boolean function  $f_T$ , how should we assign literals to the sites in a lattice such that the top-to-bottom function  $f_L$  equals  $f_T$ ? More specifically, how can we assign literals such that the OR of all the top-to-bottom paths equals  $f_T$ ? In order to solve this problem we exploit the concept of lattice duality, and work with both the target Boolean function and its dual.

Suppose that we are given a target Boolean function  $f_T$  and its dual  $f_T^D$ , both in ISOP form such that

$$f_T = P_1 + P_2 + \dots + P_n \quad \text{and} \\ f_T^D = P'_1 + P'_2 + \dots + P'_m$$

where each  $P_i$  is a prime implicant of  $f_T$ ,  $i = 1, \dots, n$ , and each  $P'_j$  is a prime implicant of  $f_T^D$ ,  $j = 1, \dots, m$ .<sup>†</sup> We use a set representation for the prime implicants:

$$P_i \rightarrow SP_i, \quad i = 1, 2, \dots, n \\ P'_j \rightarrow SP'_j, \quad j = 1, 2, \dots, m$$

where each  $SP_i$  is the set of literals in the corresponding product  $P_i$  and each  $SP'_j$  is the set of literals in the corresponding product  $P'_j$ .

#### 3.1 Algorithm

We first present the synthesis algorithm; then we illustrate it with examples; then we explain why it works.

Above we argued that, in establishing the Boolean function that a lattice implements, we must consider all possible paths. Paradoxically, our method allows us to consider only the *column paths* and the *row paths*, that is to say, the paths formed by straight-line connections

<sup>†</sup>. Here ' is used to distinguish symbols. It does *not* indicate negation.

between the top and bottom plates and between the left and right plates, respectively. Our algorithm is formulated in terms of the set representation of products and their intersections.

- 1) Begin with  $f_T$  and its dual  $f_T^D$ , both in ISOP form. Suppose that  $f_T$  and  $f_T^D$  have  $n$  and  $m$  products, respectively.
- 2) Start with an  $m \times n$  lattice. Assign each product of  $f_T$  to a column and each product of  $f_T^D$  to a row.
- 3) Compute intersection sets for every site, as shown in Figure 11.
- 4) Arbitrarily select a literal from an intersection set and assign it to the corresponding site.

The proposed implementation technique is illustrated in Figure 11. The technique implements  $f_T$  with an  $m \times n$  lattice where  $n$  and  $m$  are the number of products of  $f_T$  and  $f_T^D$ , respectively. Each of the  $n$  column paths implements a product of  $f_T$  and each of the  $m$  row paths implements a product of  $f_T^D$ . As we explain in the next section, the resulting lattice implements  $f_T$  and  $f_T^D$  as the top-to-bottom and left-to-right functions, respectively. None of the paths other than the column and row paths need be considered.

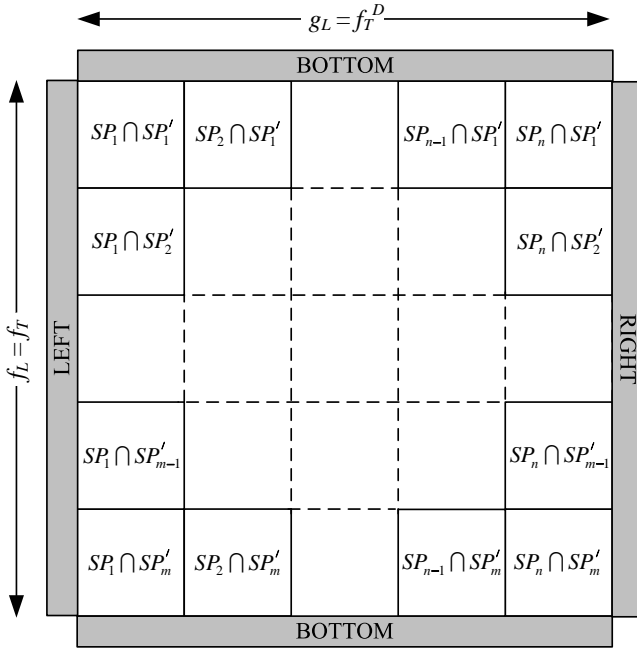


Fig. 11: Proposed implementation technique.

We present a few examples to elucidate our algorithm.

**Example 2** Suppose that we are given the following target function  $f_T$  in ISOP form:

$$f_T = x_1x_2 + x_1x_3 + x_2x_3.$$

We compute its dual  $f_T^D$  in ISOP form:

$$f_T^D = (x_1 + x_2)(x_1 + x_3)(x_2 + x_3),$$

$$f_T^D = x_1x_2 + x_1x_3 + x_2x_3.$$

We have:

$$SP_1 = \{x_1, x_2\}, \quad SP_2 = \{x_1, x_3\}, \quad SP_3 = \{x_2, x_3\},$$

$$SP'_1 = \{x_1, x_2\}, \quad SP'_2 = \{x_1, x_3\}, \quad SP'_3 = \{x_2, x_3\}.$$

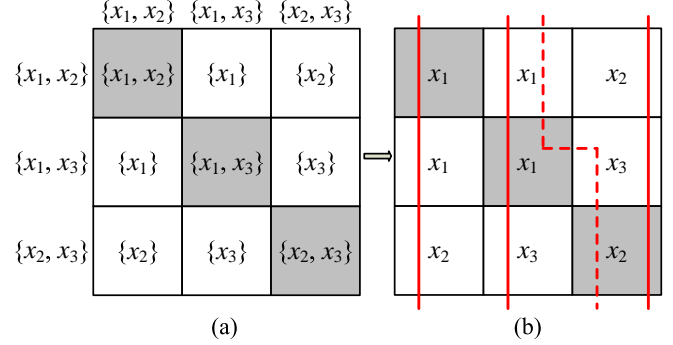


Fig. 12: Implementing  $f_T = x_1x_2 + x_1x_3 + x_2x_3$ . (a): Lattice sites with corresponding sets. (b): Lattice sites with corresponding literals.

Figure 12 shows the implementation of the target function. Grey sites represent sets having more than one literal; which literal is selected for these sites is arbitrary. For example, selecting  $x_2, x_3, x_3$  instead of  $x_1, x_1, x_2$  does not change  $f_L$  and  $g_L$ . In order to implement the target function, we only use column paths; these are shown by the solid lines. All other paths are, in fact, redundant. Indeed there are a total of 9 top-to-bottom paths: the 3 column paths and 6 other paths; however all other paths are covered by the column paths. For example, the path  $x_1x_2x_3$  shown by the dashed line is a redundant path covered by the column paths. The lattice implements the top-to-bottom and left-to-right functions  $f_L = f_T = x_1x_2 + x_1x_3 + x_2x_3$  and  $g_L = f_T^D = x_1x_2 + x_1x_3 + x_2x_3$ , respectively.

**Example 3** Suppose that we are given the following target function  $f_T$  in ISOP form:

$$f_T = x_1x_2x_3 + x_1x_4 + x_1x_5.$$

We compute its dual  $f_T^D$  in ISOP form:

$$f_T^D = (x_1)(x_2 + x_4 + x_5)(x_3 + x_4 + x_5).$$

$$f_T^D = x_1 + x_2x_4x_5 + x_3x_4x_5.$$

We have:

$$SP_1 = \{x_1, x_2, x_3\}, \quad SP_2 = \{x_1, x_4\}, \quad SP_3 = \{x_1, x_5\},$$

$$SP'_1 = \{x_1\}, \quad SP'_2 = \{x_2, x_4, x_5\}, \quad SP'_3 = \{x_3, x_4, x_5\}.$$

Figure 13 shows the implementation of the target function. In this example, all the intersection sets are singletons, so the choice of which literal to assign is clear. The lattice implements  $f_L = f_T = x_1x_2x_3 + x_1x_4 + x_1x_5$  and  $g_L = f_T^D = x_1 + x_2x_4x_5 + x_3x_4x_5$ .

We give another example, this one somewhat more complicated.

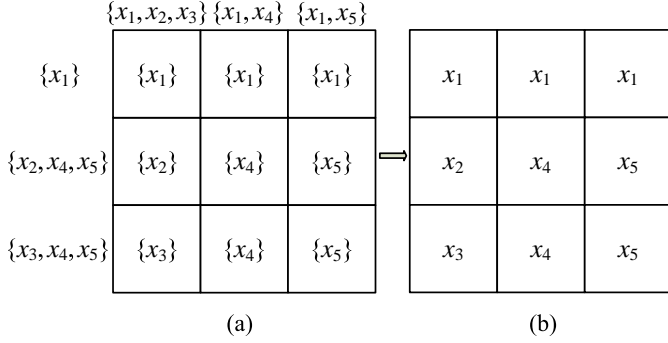


Fig. 13: Implementing  $f_T = x_1x_2x_3 + x_1x_4 + x_1x_5$ . (a): Lattice sites with corresponding sets. (b): Lattice sites with corresponding literals.

**Example 4** Suppose that  $f_T$  and  $f_T^D$  are both given in ISOP form as follows:

$$f_T = x_1\bar{x}_2x_3 + x_1\bar{x}_4 + x_2x_3\bar{x}_4 + x_2x_4x_5 + x_3x_5 \quad \text{and}$$

$$f_T^D = x_1x_2x_5 + x_1x_3x_4 + x_2x_3\bar{x}_4 + \bar{x}_2\bar{x}_4x_5.$$

	$\bar{x}_1$	$\bar{x}_2$	$x_3$	$x_4$	$x_5$
$x_1$	$x_1$	$x_1$	$x_2$	$x_2$	$x_5$
$x_1x_2x_5$	$x_1$	$x_1$	$x_2$	$x_2$	$x_5$
$x_1x_3x_4$	$x_1$	$x_1$	$x_3$	$x_4$	$x_3$
$x_2x_3\bar{x}_4$	$x_3$	$\bar{x}_4$	$x_2$	$x_2$	$x_3$
$\bar{x}_2\bar{x}_4x_5$	$\bar{x}_2$	$\bar{x}_4$	$\bar{x}_4$	$x_5$	$x_5$

Fig. 14: Implementing  $f_T = x_1\bar{x}_2x_3 + x_1\bar{x}_4 + x_2x_3\bar{x}_4 + x_2x_4x_5 + x_3x_5$ .

Figure 14 shows the implementation of the target function. Grey sites represent intersection sets having more than one literal. For these sites, selection of the final literal is arbitrary. The result is  $f_L = f_T = x_1\bar{x}_2x_3 + x_1\bar{x}_4 + x_2x_3\bar{x}_4 + x_2x_4x_5 + x_3x_5$  and  $g_L = f_T^D = x_1x_2x_5 + x_1x_3x_4 + x_2x_3\bar{x}_4 + \bar{x}_2\bar{x}_4x_5$ .

### 3.2 Proof of Correctness

We present a proof of correctness of the synthesis method. Since our method does not enumerate paths, we must answer the question: for the top-to-bottom lattice function, how do we know that all paths other than the column paths are redundant? The following theorem answers this question. It pertains to the lattice functions and their duals.

**Theorem 1** If we can find two dual functions  $f$  and  $f^D$  that are implemented as subsets of all top-to-bottom and left-to-right paths, respectively, then  $f_L = f$  and  $g_L = f^D$ .

Before presenting the proof, we provide some examples to elucidate the theorem.

**Example 5** We analyze the two lattices shown in Figure 15.

**Lattice (a):** The top-to-bottom paths shown by the red lines implement  $f = x_1x_2 + \bar{x}_1x_3$ . The left-to-right paths shown by the blue lines implement  $g = x_1x_3 + \bar{x}_1x_2$ . Since  $g = f^D$ , we can apply Theorem 1:  $f_L = f = x_1x_2 + \bar{x}_1x_3$  and  $g_L = f^D = x_1x_3 + \bar{x}_1x_2$ . Relying on the theorem, we obtain the functions without examining all possible paths. Let us check the result by using the formal definition of  $f_L$  and  $g_L$ , namely the OR of all corresponding paths. Since there are 9 total top-to-bottom paths,  $f_L = x_1x_1\bar{x}_1 + x_1x_1x_2x_2 + x_1x_1x_2x_3\bar{x}_1 + x_3x_2x_1\bar{x}_1 + x_3x_2x_2 + x_3x_2x_3\bar{x}_1 + x_3x_3\bar{x}_1 + x_3x_3x_2x_2 + x_3x_3x_2x_1\bar{x}_1$ , which is equal to  $x_1x_2 + \bar{x}_1x_3$ . Thus all the top-to-bottom paths but the paths shown by the red lines are redundant. Since there are 9 total left-to-right paths,  $g_L = x_1x_3x_3 + x_1x_3x_2x_3 + x_1x_3x_2x_2\bar{x}_1 + x_1x_2x_3x_3 + x_1x_2x_3 + x_1x_2x_2\bar{x}_1 + \bar{x}_1x_2x_2x_3x_3 + \bar{x}_1x_2x_2x_3 + \bar{x}_1x_2\bar{x}_1$ , which is equal to  $x_1x_3 + \bar{x}_1x_2$ . Thus all the left-to-right paths but the paths shown by the blue lines are redundant. So Theorem 1 holds for this example.

**Lattice (b):** The top-to-bottom paths shown by the red lines implement  $f = x_1x_2x_3 + x_1x_4 + x_1x_5$ . The left-to-right paths shown by the blue lines implement  $g = x_1 + x_2x_4x_5 + x_3x_4x_5$ . Since  $g = f^D$ , we can apply Theorem 1:  $f_L = f = x_1x_2x_3 + x_1x_4 + x_1x_5$  and  $g_L = f^D = x_1 + x_2x_4x_5 + x_3x_4x_5$ . Again, we see that Theorem 1 holds for this example.

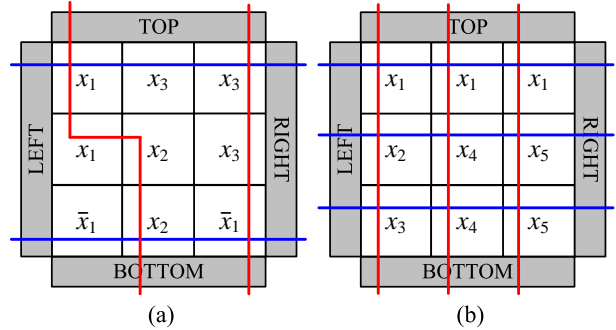


Fig. 15: Examples to illustrate Theorem 1.

*Proof of Theorem 1:* If  $f(x_1, x_2, \dots, x_k) = 1$  then  $f_L = 1$ . From the definition of duality, if  $f(x_1, x_2, \dots, x_k) = 0$  then  $g(\bar{x}_1, \bar{x}_2, \dots, \bar{x}_k) = \bar{f}(x_1, x_2, \dots, x_k) = 1$ . This means that there is a left-to-right path consisting of all 0's; accordingly,  $f_L = 0$ . Thus, we conclude that  $f_L = f$ . Following the same argument for  $g$ , we conclude that  $g_L = f^D$ .  $\square$

Theorem 1 provides a constructive method for synthesizing lattices with the requisite property, namely that the top-to-bottom and left-to-right functions  $f_T$  and  $f_T^D$  are duals, and each column path of the lattice imple-

ments a product of  $f_T$  and each row path implements a product of  $f_T^D$ .

We begin by lining up the products of  $f_T$  as the column headings and the products of  $f_T^D$  as the row headings. We compute intersection sets for every lattice site. We arbitrarily select a literal from each intersection set and assign it to the corresponding site. The following lemma and theorem explain why we can make such an arbitrary selection.

Suppose that functions  $f(x_1, x_2, \dots, x_k)$  and  $f^D(x_1, x_2, \dots, x_k)$  are both given in ISOP form such that

$$\begin{aligned} f &= P_1 + P_2 + \dots + P_n & \text{and} \\ f^D &= P'_1 + P'_2 + \dots + P'_m \end{aligned}$$

where each  $P_i$  is a prime implicant of  $f$ ,  $i = 1, \dots, n$ , and each  $P'_j$  is a prime implicant of  $f^D$ ,  $j = 1, \dots, m$ . Again, we use a set representation for the prime implicants:

$$\begin{aligned} P_i &\rightarrow SP_i, & i = 1, 2, \dots, n \\ P'_j &\rightarrow SP'_j, & j = 1, 2, \dots, m \end{aligned}$$

where each  $SP_i$  is the set of literals in the corresponding product  $P_i$  and each  $SP'_j$  is the set of literals in the corresponding product  $P'_j$ . Suppose that  $SP_i$  and  $SP'_j$  have  $z_i$  and  $z'_j$  elements, respectively. We first present a property of dual Boolean functions from [3]:

**Lemma 1** *Dual pairs  $f$  and  $f^D$  must satisfy the condition*

$$SP_i \cap SP'_j \neq \emptyset \quad \text{for every } i = 1, 2, \dots, n \text{ and } j = 1, 2, \dots, m.$$

*Proof of Lemma 1:* The proof is by contradiction. Suppose that we focus on one product  $P_i$  from  $f$  and assign all its literals, namely those in the set  $SP_i$ , to 0. In this case  $f^D = 0$ . However if there is a product  $P'_j$  of  $f^D$  such that  $SP'_j \cap SP_i = \emptyset$ , then we can always make  $P'_j$  equal 1 because  $SP'_j$  does not contain any literals that have been previously assigned to 0. It follows that  $f^D = 1$ , a contradiction.  $\square$

**Lemma 2** *Consider a product  $P$  with a corresponding set representation  $SP$ . Consider a Boolean function  $f = P_1 + P_2 + \dots + P_n$  with a corresponding set representation  $SP_i$  for each of its products  $P_i$ ,  $i = 1, 2, \dots, n$ . If  $SP$  has non-empty intersections with every  $SP_i$ ,  $i = 1, 2, \dots, n$ , then  $P$  is a product of  $f^D$ .*

*Proof of Lemma 2:* To prove that  $P$  is a product of  $f^D$  we assign 1's to all the variables of  $P$  and see if this always results in  $f^D = 1$ . Since  $SP$  has non-empty intersections with every  $SP_i$ ,  $i = 1, 2, \dots, n$ , each product of  $f$  should have at least one assigned 1. From the definition of duality, these assigned 1's always result in  $f^D = (1 + \dots)(1 + \dots) \dots (1 + \dots) = 1$ .  $\square$

**Theorem 2** *Assume that  $f$  and  $f^D$  are both in ISOP form. For any product  $P_i$  of  $f$ , there exist  $m$  non-empty intersection sets,  $(SP_i \cap SP'_1), (SP_i \cap SP'_2), \dots, (SP_i \cap SP'_m)$ . Among these  $m$  sets, there must be at least  $z_i$  single-element disjoint*

*sets. These single-element sets include all  $z_i$  literals of  $P_i$ .*

*We can make the same claim for products of  $f^D$ : for any product  $P'_j$  of  $f^D$  there exist  $n$  non-empty intersection sets,  $(SP'_j \cap SP_1), (SP'_j \cap SP_2), \dots, (SP'_j \cap SP_n)$ . Among these  $n$  sets there must be at least  $z'_j$  single-element disjoint sets that each represents one of the  $z'_j$  literals of  $P'_j$ .*

Before proving the theorem we elucidate it with examples.

**Example 6** *Suppose that we are given a target function  $f_T$  and its dual  $f_T^D$ , both in ISOP form such that*

$$f_T = x_1 \bar{x}_2 + \bar{x}_1 x_2 x_3 \quad \text{and} \quad f_T^D = x_1 x_2 + x_1 x_3 + \bar{x}_1 \bar{x}_2.$$

*Thus,*

$$\begin{aligned} SP_1 &= \{x_1, \bar{x}_2\}, & SP_2 &= \{\bar{x}_1, x_2, x_3\}, \\ SP'_1 &= \{x_1, x_2\}, & SP'_2 &= \{x_1, x_3\}, & SP'_3 &= \{\bar{x}_1, \bar{x}_2\}. \end{aligned}$$

*Let us apply Theorem 2 for  $SP_2$  ( $z_2 = 3$ ).*

$$SP_2 \cap SP'_1 = \{x_2\}, \quad SP_2 \cap SP'_2 = \{x_3\}, \quad SP_2 \cap SP'_3 = \{\bar{x}_1\}.$$

*Since these three sets are all the single-element disjoint sets of the literals of  $SP_2$ , Theorem 2 is satisfied.*

**Example 7** *Suppose that we are given a target function  $f_T$  and its dual  $f_T^D$ , both in ISOP form such that*

$$f_T = x_1 x_2 + x_1 x_3 + x_2 x_3 \quad \text{and} \quad f_T^D = x_1 x_2 + x_1 x_3 + x_2 x_3.$$

*Thus,*

$$\begin{aligned} SP_1 &= \{x_1, x_2\}, & SP_2 &= \{x_1, x_3\}, & SP_3 &= \{x_2, x_3\}, \\ SP'_1 &= \{x_1, x_2\}, & SP'_2 &= \{x_1, x_3\}, & SP'_3 &= \{x_2, x_3\}. \end{aligned}$$

*Let us apply Theorem 2 for  $SP'_1$  ( $z'_1 = 2$ ).*

$$SP'_1 \cap SP_1 = \{x_1, x_2\}, \quad SP'_1 \cap SP_2 = \{x_1\}, \quad SP'_1 \cap SP_3 = \{x_2\}.$$

*Since  $\{x_1\}$  and  $\{x_2\}$ , the single-element disjoint sets of the literals of  $SP'_1$ , are among these sets, Theorem 2 is satisfied.*

*Proof of Theorem 2:* The proof is by contradiction. Consider a product  $P_i$  of  $f$  such that  $SP_i = \{x_1, x_2, \dots, x_{z_i}\}$ . From Lemma 1 we know that  $SP_i$  has non-empty intersections with every  $SP'_j$ ,  $j = 1, 2, \dots, m$ . For one of the elements of  $SP_i$ , say  $x_1$ , assume that none of the intersection sets  $(SP_i \cap SP'_1), (SP_i \cap SP'_2), \dots, (SP_i \cap SP'_m)$  is  $\{x_1\}$ . This means that if we extract  $x_1$  from  $SP_i$  then the new set  $\{x_2, \dots, x_{z_i}\}$  also has non-empty intersections with every  $SP'_j$ ,  $j = 1, 2, \dots, m$ . From Lemma 2 we know that the product  $x_2 x_3 \dots x_{z_i}$  must be a product of  $f$ . This product covers  $P_i$ . However, in an ISOP expression, all products including  $P_i$  are irredundant, not covered by a product of  $f$ . So we have a contradiction.  $\square$

From Lemma 1 we know that none of the lattice sites will have an empty intersection set. Theorem 2 states that the intersection sets of a product include single-element sets for all of its literals. So the corresponding column

or row has always all literals of the product regardless of the final literal selections from multiple-element sets. Thus we obtain a lattice whose column paths and row paths implement  $f_T$  and  $f_T^D$ , respectively.

#### 4 PARITY FUNCTIONS

The algorithm proposed in Section 3 provides a general method for implementing any type of Boolean function with an  $m \times n$  lattice, where  $n$  and  $m$  are the number of products of the function and its dual, respectively. In this section, we discuss a method for implementing a specific function, the *parity function*, with a  $(\log(m)+1) \times n$  lattice. Compared to the general method, we improve the lattice size by a factor of  $m/(\log(m)+1)$  for this function.

As defined in Section 1.1, a  $k$ -variable parity function can be represented as a  $k$ -variable  $XOR$  operation. We exploit the following properties of  $XOR$  functions:

$$\begin{aligned} XOR_k &= x_k \overline{XOR}_{k-1} + \bar{x}_k XOR_{k-1} \\ \overline{XOR}_k &= x_k XOR_{k-1} + \bar{x}_k \overline{XOR}_{k-1}. \end{aligned}$$

These properties allow us to implement both  $XOR_k$  and its complement  $\overline{XOR}_k$  recursively. The approach for the  $k$ -variable parity function is illustrated in Figure 16. The approach for 1, 2, and 3 variable parity functions is shown in Figure 17. As in our general method, we implement each product of the target function with a separate column path; in this construction, all paths other than column paths are redundant. The following lemma explains why this configuration works. Figure 18 illustrates the lemma.

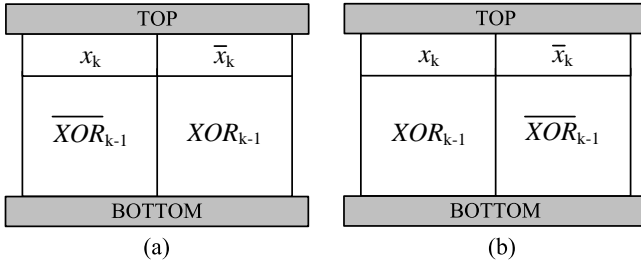


Fig. 16: (a): Implementation of  $XOR_k$ . (b): Implementation of  $\overline{XOR}_k$ .

**Lemma 3** Consider two lattices with the same number of rows. Suppose that the lattices implement the Boolean functions  $f_{L1}$  and  $f_{L2}$ . Construct a new lattice with the two lattices side by side. If the attached columns of the lattices have negated variables facing each other for all rows except the first and the last, then the new lattice implements the Boolean function  $f_{L3} = f_{L1} + f_{L2}$ .

*Proof of Lemma 3:* The new lattice has three types of paths: paths having all sites from the first lattice that implement  $f_{L1}$ , paths having all sites from the second lattice that implement  $f_{L2}$ , and paths having sites from both the first and the second lattices that implement

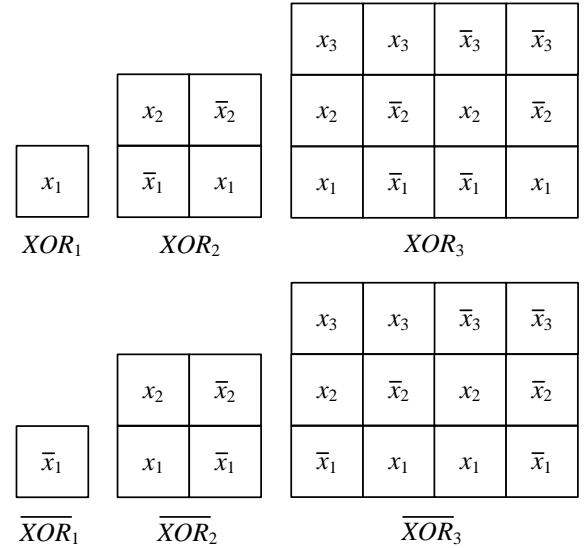


Fig. 17: Implementation of  $XOR_1$ ,  $\overline{XOR}_1$ ,  $XOR_2$ ,  $\overline{XOR}_2$ ,  $XOR_3$ , and  $\overline{XOR}_3$ .

$f_{L1-2}$ . The Boolean function  $f_{L3}$  implemented by the third lattice is OR of the all paths;  $f_{L3} = f_{L1} + f_{L2} + f_{L1-2}$ . Since negated variables in attached columns result in  $f_{L1-2} = 0$ , we conclude that  $f_{L3} = f_{L1} + f_{L2}$ .  $\square$

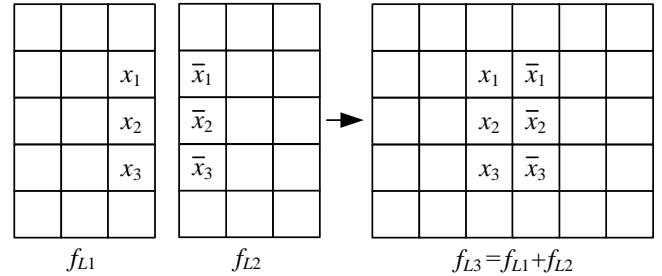


Fig. 18: An example illustrating Lemma 3.

We exploit Lemma 3 to compute the parity function as follows (please refer back to Figure 16). We attach the lattices implementing  $f_{L1} = x_k \overline{XOR}_{k-1}$  and  $f_{L2} = \bar{x}_k XOR_{k-1}$  to implement  $f_{L3} = XOR_k$ . We attach the lattices implementing  $f_{L1} = x_k XOR_{k-1}$  and  $f_{L2} = \bar{x}_k \overline{XOR}_{k-1}$  to implement  $f_{L3} = \overline{XOR}_k$ . One can easily see that attached columns always have the proper configuration of negated variables to ensure that  $f_{L1-2} = 0$ .

#### 5 A LOWER BOUND ON THE LATTICE SIZE

In this section, we propose a lower bound on the size of any lattice implementing a Boolean function. Although it is a weak lower bound, it allows us to gauge the effectiveness of our synthesis method. The bound is predicated on the maximum length of any path across the lattice. The length of such a path is bounded from below by the maximum number of literals in terms of an ISOP expression for the function.

## 5.1 Preliminaries

**Definition 7** Let the **degree** of an SOP expression be the maximum number of literals in terms of the expression.

A Boolean function might have several different ISOP expressions and these might have different degrees. Among all the different expressions, we need the one with the smallest degree for our lower bound. (We need only consider ISOP expressions; every SOP expression is covered by an ISOP expression of equal or lesser degree.)

Consider a target Boolean function  $f_T$  and its dual  $f_T^D$ , both in ISOP form. We will use  $v$  and  $y$  to denote the minimum degrees of  $f_T$  and  $f_T^D$ , respectively. For example, if  $v = 3$  and  $y = 5$ , this means that every ISOP expression for  $f_T$  includes terms with 3 literals or more, and every ISOP expression for  $f_T^D$  includes terms with 5 literals or more. Our lower bound, described in the next section by Theorem 4, consists of inequalities on  $v$  and  $y$ . We first illustrate how it works with an example.

**Example 8** Consider two target Boolean functions  $f_{T1} = x_1x_2x_3 + x_1x_4 + x_1x_5$  and  $f_{T2} = x_1x_2x_3 + \bar{x}_1\bar{x}_2x_4 + x_2x_3x_4$ , and their duals  $f_{T1}^D = x_1 + x_2x_4x_5 + x_3x_4x_5$  and  $f_{T2}^D = x_1x_4 + \bar{x}_1x_2 + \bar{x}_2x_3$ . These expressions are all in ISOP form with minimum degrees. Since each expressions consists of three products, the synthesis method described in Section 3 implements each target function with a  $3 \times 3$  lattice.

Examining the expressions, we see that the degrees of  $f_{T1}$  and  $f_{T2}$  are  $v_1 = 3$  and  $v_2 = 3$ , respectively, and the degrees of  $f_{T1}^D$  and  $f_{T2}^D$  are  $y_1 = 3$  and  $y_2 = 2$ , respectively. Our lower bounds based on these values are  $3 \times 3$  for  $f_{T1}$  and  $3 \times 2$  for  $f_{T2}$ . Thus, the lower bound for  $f_{T2}$  suggests that our synthesis method might not be producing optimal results. Indeed, Figure 19 shows minimum-sized lattices for for  $f_{T1}$  and  $f_{T2}$ . Here the  $3 \times 2$  lattice for  $f_{T2}$  was obtained through exhaustive search.

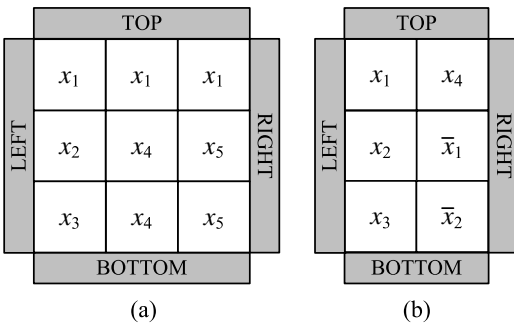


Fig. 19: Minimum-sized lattices (a):  $f_L = f_{T1} = x_1x_2x_3 + x_1x_4 + x_1x_5$ . (b):  $f_L = f_{T2} = x_1x_2x_3 + \bar{x}_1\bar{x}_2x_4 + x_2x_3x_4$ .

Since we implement Boolean functions in terms of top-to-bottom connectivity across the lattice, it is apparent that we cannot implement a target function  $f_T$  with top-to-bottom paths consisting of fewer than  $v$  literals, where  $v$  is the minimum degree of an ISOP expression for  $f_T$ . The following theorem explains the role of  $y$ , the

minimum degree of  $f_T^D$ . It is based on *eight-connected* paths.<sup>1</sup>

**Definition 8** An **eight-connected path** consists of both *directly* and *diagonally adjacent* sites.

An example is shown in Figure 20. Here the paths  $x_1x_4x_8$  and  $x_3x_6x_5x_8$  shown by red and blue lines are both eight-connected paths; however only the blue one is four-connected.

Recall that  $f_L$  and  $g_L$  are defined as the OR of all four-connected top-to-bottom and left-to-right paths, respectively. (A lattice implements a given target function  $f_T$  if  $f_L = f_T$ .) We define  $f_{L-8}$  and  $g_{L-8}$  to be the OR of all eight-connected top-to-bottom and left-to-right paths, respectively.

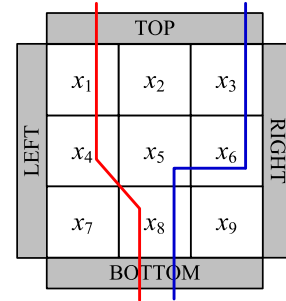


Fig. 20: A lattice with eight-connected paths.

**Theorem 3** The functions  $f_L$  and  $g_{L-8}$  are duals. The functions  $f_{L-8}$  and  $g_L$  duals.

Before proving the theorem, we elucidate it with an example.

**Example 9** Consider the lattice shown in Figure 21. Here  $f_L$  is the OR of 3 top-to-bottom four-connected paths  $x_1x_4$ ,  $x_2x_5$ , and  $x_3x_6$ ;  $g_L$  is the OR of 4 left-to-right four-connected paths  $x_1x_2x_3$ ,  $x_1x_2x_5x_6$ ,  $x_4x_5x_2x_3$ , and  $x_4x_5x_6$ ;  $f_{L-8}$  is the OR of 7 eight-connected top-to-bottom paths  $x_1x_4$ ,  $x_1x_5$ ,  $x_2x_4$ ,  $x_2x_5$ ,  $x_2x_6$ ,  $x_3x_5$ , and  $x_3x_6$ ; and  $g_{L-8}$  is the OR of 8 eight-connected left-to-right paths  $x_1x_2x_3$ ,  $x_1x_2x_6$ ,  $x_1x_5x_3$ ,  $x_1x_5x_6$ ,  $x_4x_2x_3$ ,  $x_4x_2x_6$ ,  $x_4x_5x_3$ , and  $x_4x_5x_6$ . We can easily verify that  $f_L = g_{L-8}^D$  and  $f_{L-8} = g_L^D$ . Accordingly, Theorem 3 holds true for this example.

*Proof of Theorem 3:* We consider two cases, namely  $f_L = 1$  and  $f_L = 0$ .

**Case 1:** If  $f_L(x_1, x_2, \dots, x_k) = 1$ , there must be a four-connected path of 1's between the top and bottom plates. If we complement all the inputs ( $1 \rightarrow 0, 0 \rightarrow 1$ ), these four-connected 1's become 0's and vertically separate the lattice into two parts. Therefore no eight-connected path of 1's exists between the left and right

1. Note that because our synthesis methodology is based on lattices of four-terminal switches, the target function  $f_T$  is always implemented by four-connected paths. We discuss eight-connected paths only because it is helpful to do so in order to prove our lower bound.

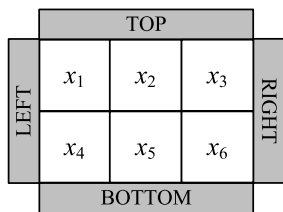
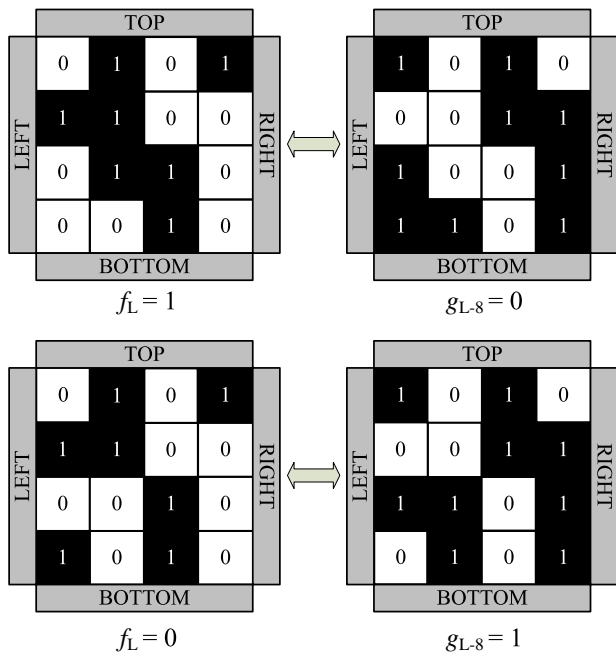
Fig. 21: A  $2 \times 3$  lattice with assigned literals.

Fig. 22: Conceptual proof of Theorem 3.

plates; accordingly,  $g_{L-8}(\bar{x}_1, \bar{x}_2, \dots, \bar{x}_k) = 0$ . As a result  $\bar{g}_{L-8}(\bar{x}_1, \bar{x}_2, \dots, \bar{x}_k) = f_L(x_1, x_2, \dots, x_k) = 1$

**Case 2:** If  $f_L(x_1, x_2, \dots, x_k) = 0$ , there must be an eight-connected path of 0's between the left and right plates. If we complement all the inputs, these eight-connected 0's become 1's; accordingly,  $g_{L-8}(\bar{x}_1, \bar{x}_2, \dots, \bar{x}_k) = 1$ . As a result  $\bar{g}_{L-8}(\bar{x}_1, \bar{x}_2, \dots, \bar{x}_k) = f_L(x_1, x_2, \dots, x_k) = 0$

Figure 22 illustrates the two cases. Taken together, the two cases prove that  $f_L$  and  $g_{L-8}$  are duals. With inverse reasoning we can prove that  $f_{L-8}$  and  $g_L$  are duals.  $\square$

Theorem 3 tells us that the products of  $f_T^D$  are implemented with eight-connected left-to-right paths. Now consider  $y$ , the degree of  $f_T^D$ . We know that we cannot implement  $f_T^D$  with eight-connected right-to-left paths having fewer than  $y$  literals. Consider  $v$ , the degree of  $f_T$ . We know that we cannot implement  $f_T$  with four-connected top-to-bottom paths having fewer than  $v$  literals.

Returning to the functions in Example 8, we can now prove that lower bounds on the lattice sizes are 9 ( $3 \times 3$ ) for  $f_{T1}$ , and 6 ( $3 \times 2$ ) for  $f_{T2}$ . Since  $v_1 = 3$  and  $y_1 = 3$  for  $f_{T1}$ , a  $3 \times 3$  lattice is a minimum-size lattice that has

four-connected top-to-bottom and eight-connected left-to-right paths of at least 3 literals, respectively. Since  $v_2 = 3$  and  $y_2 = 2$  for  $f_{T2}$ , a  $3 \times 2$  lattice is a minimum-size lattice that has four-connected top-to-bottom and eight-connected left-to-right paths of at least 3 and 2 literals, respectively.

Based on these preliminaries, we now formulate the lower bound.

## 5.2 Lower Bound

Consider a target Boolean function  $f_T$  and its dual  $f_T^D$ , both in ISOP form. Recall that  $v$  and  $y$  are defined as the minimum degrees of  $f_T$  and  $f_T^D$ , respectively. Our lower bound is based on the observation that a minimum-size lattice must have a four-connected top-to-bottom path with at least  $v$  literals and an eight-connected left-to-right path with at least  $y$  literals. Since the functions are in ISOP form, all products of  $f_T$  and  $f_T^D$  are irredundant, i.e., not covered by other products. Therefore, we need only to consider irredundant paths:

**Definition 9** A four-connected (eight-connected) path between plates is **irredundant** if it is not covered by another four-connected (eight-connected) path between the corresponding plates.

We bound the length of irredundant paths. For example, the length of an eight-connected left-to-right path in a  $3 \times 3$  lattice is at most 3. Accordingly, no Boolean function with  $y$  greater than 3 can be implemented by a  $3 \times 3$  lattice. Figure 23 shows eight-connected left-to-right paths in a  $3 \times 3$  lattice. The path in (a) consists of 3 sites. The path in (b) consists of 4 sites; however it is a redundant path – it is covered by the path in (a).

The following simple lemmas pertain to irredundant paths of a lattice.

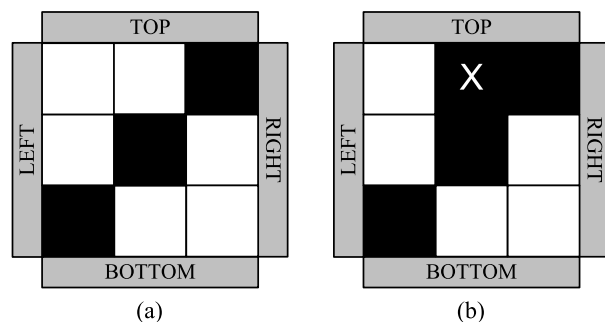


Fig. 23: Lattices with (a) an irredundant path and (b) a redundant path.

**Lemma 4** An irredundant top-to-bottom path of a lattice contains exactly one site from the topmost row and exactly one site from the bottommost row. An irredundant left-to-right path of a lattice contains exactly one site from the leftmost column and exactly one site from the rightmost column.

*Proof of Lemma 4:* All sites in the first row of a lattice are connected through the top plate. Therefore we do not need a path to connect any two sites in this row; such a path is redundant. Similarly for the last row. Similarly for the first and last columns.  $\square$

**Lemma 5** *An irredundant four-connected path of a lattice contains at most 3 of 4 sites in any  $2 \times 2$  sub-lattice. An irredundant eight-connected path of a lattice contains at most 2 of 4 sites in any  $2 \times 2$  sub-lattice.*

*Proof of Lemma 5:* In order to connect any 2 sites of a  $2 \times 2$  sub-lattice with a four-connected path, we need at most 3 sites of the sub-lattice. Similarly, in order to connect any 2 sites of a  $2 \times 2$  sub-lattice with an eight-connected path, we need at most 2 sites of the sub-lattice.  $\square$

Figure 24 shows examples illustrating Lemma 5. The lattice in (a) has a four-connected top-to-bottom path. This path contains 4 of the 4 sites in the  $2 \times 2$  sub-lattice encircled in red. Lemma 5 tells us that the path in (a) is redundant. Indeed, it is covered by the path achieved by removing the site marked by  $\times$ . The lattice in (b) has an eight-connected left-to-right path. This path contains 3 of 4 sites in the  $2 \times 2$  sub-lattice encircled in red. Lemma 5 tells us that the path in (b) is redundant. Indeed it is covered by the path achieved by removing the site marked by  $\times$ .

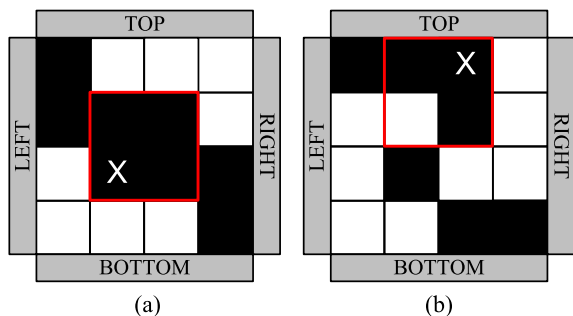


Fig. 24: Examples to illustrate Lemma 5.

From Lemmas 4 and 5, we have the following theorem consisting of two inequalities. The first inequality states that the degree of  $f_T$  is equal to or less than the maximum number of sites in any four-connected top-to-bottom path. The second inequality states that the degree of  $f_T^D$  is less than or equal to the maximum number of sites in any eight-connected left-to-right path.

**Theorem 4** *If a target Boolean function  $f_T$  is implemented by an  $R \times C$  lattice then the following inequalities must be satisfied:*

$$v \leq \begin{cases} R, & \text{if } R \leq 2 \text{ or } C \leq 1 \\ 3 \left\lceil \frac{R-2}{2} \right\rceil \left\lceil \frac{C}{2} \right\rceil + \frac{2+(-1)^R+(-1)^C}{2}, & \text{if } R > 2 \text{ and } C > 1, \end{cases}$$

$$y \leq \begin{cases} C, & \text{if } R \leq 3 \text{ or } C \leq 2 \\ 2 \left\lceil \frac{R}{2} \right\rceil \left\lceil \frac{C-2}{2} \right\rceil + \frac{2+(-1)^R+(-1)^C}{2}, & \text{if } R > 3 \text{ and } C > 2, \end{cases}$$

where  $v$  and  $y$  are the minimum degrees of  $f_T$  and its dual  $f_T^D$ , respectively, both in ISOP form.

*Proof of Theorem 4:* If  $R$  and  $C$  are both even then all irredundant top-to-bottom and left-to-right paths contain at most  $\frac{3}{4}(R-2)C+2$  and  $\frac{2}{4}R(C-2)+2$  sites, respectively; this follows directly from Lemmas 4 and 5. If  $R$  or  $C$  are odd then we first round these up to the nearest even number. The resulting lattice contains at least one extra site (if either  $R$  or  $C$  but not both are odd) or two extra sites (if both  $R$  and  $C$  are odd). Accordingly, we compute the maximum number of sites in top-to-bottom and left-to-right paths and subtract 1 or 2. This calculation is reflected in the inequalities.  $\square$

The theorem proves our lower bound. Table 1 shows the calculation of the bound for different values of  $v$  and  $y$  up to 10.

$v \backslash y$	1	2	3	4	5	6	7	8	9	10
1	1	2	3	4	5	6	7	8	9	10
2	2	4	6	8	10	12	14	16	18	20
3	3	6	9	12	12	15	20	20	20	24
4	4	6	9	12	12	15	20	20	20	24
5	5	8	9	12	12	15	20	20	20	24
6	6	9	9	12	12	15	20	20	20	24
7	7	10	12	12	12	15	20	20	20	24
8	8	12	15	15	15	15	20	20	20	24
9	9	14	15	15	15	15	20	20	20	24
10	10	14	15	15	15	15	20	20	20	24

TABLE 1: Lower bounds on the lattice size for different values of  $v$  and  $y$ .

## 6 EXPERIMENTAL RESULTS

In Table 2 we report synthesis results for a few standard benchmark circuits [18]. We treat each output of a benchmark circuit as a separate target function.

The values for  $n$  and  $m$  represent the number of products for each target function  $f_T$  and its dual  $f_T^D$ , respectively. We obtained these through sum-of-products minimization using the program Espresso [20]. The lattice size, representing the number of switches, is computed as a product of  $n$  and  $m$ .

For the lower bound calculation, we obtained values of  $v$  and  $y$ , the minimum degrees of  $f_T$  and  $f_T^D$ , as follows: first we generated prime implicant tables for the target functions and their duals using Espresso with the “-Dprimes” option; then we deleted prime implicants one by one, beginning with those that had the most literals, until we obtained an expression of minimum degree. Given values of  $v$  and  $y$ , we computed the lower bound from the inequalities in Theorem 4.

Table 2 lists the runtimes for the lattice size and the lower bound calculations. The runtimes for the lattice size consist of the time for obtaining the functions' duals and for SOP minimization of both the functions and their duals. The runtimes for the lower bound consist of the time for generating the prime implicant tables and for obtaining the minimum degrees from the tables. We performed trials on an AMD Athlon 64 X2 6000+ Processor (at 3Ghz) with 3.6GB of RAM running Linux.

Examining the numbers in Table 2, we see that, often, the synthesized lattice size matches the lower bound. In these cases, our results are optimal. However for most of the Boolean functions, especially those with larger values of  $n$  and  $m$ , the lower bound is much smaller than the synthesized lattice size. This is not surprising since the lower bound is weak, formulated based on path lengths.

In the final column of Table 2, we list the number of transistors required in a CMOS implementation of the functions. We obtained the transistor counts through synthesis trials with the Berkeley tool ABC [19]. We applied the standard synthesis script "resyn2" in ABC and then mapped to a generic library consisting of NAND2 gates and inverters. We assume that each NAND2 gate requires four transistors and each inverter requires two transistors.

The number of switches needed by our method compares very favorably to the number of transistors required in a CMOS implementation. Of course, a rigorous comparison would depend on the specifics of the types of technology used. Each four-terminal switch might equate to more than one transistor. Then again, in some nanoscale technologies, it might equate to much less: the density of crosspoints in nanowire arrays is generally much higher than the density achievable with CMOS transistors.

## 7 DISCUSSION

The two-terminal switch model is fundamental and ubiquitous in electrical engineering [21]. Either implicitly or explicitly, nearly all logic synthesis methods target circuits built from independently controllable two-terminal switches (i.e., transistors). And yet, with the advent of novel nanoscale technologies, synthesis methods targeting lattices of multi-terminal switches are *apropos*. Our treatment is at a technology-independent level; nevertheless we comment that our synthesis results are applicable to technologies such as nanowire crossbar arrays with independently controllable crosspoints [13].

In this paper, we presented a synthesis method targeting regular lattices of four-terminal switches. Significantly, our method assigns literals to lattice sites without enumerating paths. It produces lattice sizes that are linear in the number of products of the target Boolean function. The time complexity of our synthesis algorithm is polynomial in the number of products. Comparing our results to a lower bound, we conclude that the synthesis results are not optimal. However, this is hardly

surprising: at their core, most logic synthesis problems are computationally intractable; the solutions that are available are based on heuristics. Furthermore, good lower bounds on circuit size are notoriously difficult to establish. In fact, such proofs are related to fundamental questions in computer science, such as the separation of the  $P$  and  $NP$  complexity classes. (To prove that  $P \neq NP$  it would suffice to find a class of problems in  $NP$  that cannot be computed by a polynomially sized circuit [22].)

The results on benchmarks illustrate that our method is effective for Boolean functions of practical interest. We should note, however, we would not expect it to be effective on some specific types of Boolean functions. In particular, our method will not be effective for Boolean functions that have duals with large number of products. The lattices for such functions will be inordinately large. For example, consider the function  $f = x_1x_2x_3 + x_4x_5x_6 + x_7x_8x_9 + x_{10}x_{11}x_{12} + x_{13}x_{14}x_{15} + x_{16}x_{17}x_{18}$ . It has only six products, but its dual has  $3^6 = 729$  products. With our method, a lattice with 729 rows and 6 columns would be required.

The cost of implementing such functions could be mitigated by decomposing and implementing Boolean functions with separate lattices (or physically separated regions in a single lattice). This paper did not consider the topic of sharing logic among multiple output functions. Techniques for functional decomposition are well established [20], [23]. In future work, we will explore techniques for exploiting such decompositions and logic sharing in lattice-based implementations. Implementing multiple output functions will require some kind of physical partitioning of the lattice.

Another future direction is to extend the results in this paper to lattices of eight-terminal switches, and then to  $2^k$ -terminal switches, for arbitrary  $k$ . Another direction is to study methods for synthesizing robust computation in lattices with *random connectivity*. We have been exploring methods based on the principle of *percolation* [24].

A significant tangent for this work is its mathematical contribution: lattice-based implementations present a novel view of the properties of Boolean functions. We are curious to study the applicability of these properties to the famous problem of testing whether two monotone Boolean functions in ISOP form are dual. This is one of the few problems in circuit complexity whose precise tractability status is unknown [25].

## ACKNOWLEDGMENTS

We would like to thank Ivo Rosenberg for his contributions.

## REFERENCES

- [1] M. Altun and M. D. Riedel, "Lattice-based computation of Boolean functions," in *Design Automation Conference*, 2010, pp. 609–612.

Circuit	$n$	$m$	Lattice size (number of switches)	Runtime (s)	$v$	$y$	Lower bound	Runtime (s)	CMOS circuit size (number of transistors)
alu1	3	2	6		2	3	6		18
alu1	2	3	6	< 0.01	3	2	6	0.02	26
alu1	1	3	3		3	1	3		16
clpl	4	4	16		4	4	12		42
clpl	3	3	9	< 0.01	3	3	9	0.01	26
clpl	2	2	4		2	2	4		10
clpl	6	6	36		6	6	15		74
clpl	5	5	25		5	5	12		64
newtag	8	4	32	< 0.01	3	6	15	< 0.01	60
dc1	4	4	16		3	3	9		38
dc1	2	3	6	< 0.01	3	2	6	< 0.01	24
dc1	4	4	16		3	4	12		40
dc1	4	5	20		4	3	9		42
dc1	3	3	9		2	3	6		26
misex1	2	5	10		4	2	6		64
misex1	5	7	35	< 0.01	4	4	12	0.01	84
misex1	5	8	40		5	4	12		64
misex1	4	7	28		5	3	9		58
misex1	5	5	25		4	4	12		76
misex1	6	7	42		4	4	12		64
misex1	5	7	35		4	3	9		36
ex5	1	3	3		3	1	3		16
ex5	1	5	5		5	1	5		24
ex5	1	4	4		4	1	4		18
ex5	1	7	7		7	1	7		36
ex5	1	8	8		8	1	8		40
ex5	1	6	6		6	1	6		34
ex5	8	4	32		3	6	15		46
ex5	10	4	40		3	8	20		52
ex5	7	3	21		3	7	20		44
ex5	7	3	21		3	6	15		48
ex5	8	2	16		2	8	16		42
ex5	9	4	36		3	8	20		56
ex5	8	2	16	0.26	2	7	14	3.17	42
ex5	12	6	72		4	7	20		70
ex5	14	8	112		4	7	20		388
ex5	7	2	14		2	7	14		38
ex5	6	3	18		3	6	15		40
ex5	6	2	12		2	6	12		36
ex5	10	7	70		3	7	20		76
ex5	6	6	36		3	6	15		64
ex5	12	10	120		4	8	20		318
ex5	14	8	112		5	7	20		350
ex5	8	5	40		3	7	20		86
ex5	10	8	80		3	7	20		116
ex5	12	7	84		4	7	20		356
ex5	9	3	27		3	8	20		60
ex5	5	2	10		2	5	10		44
b12	4	6	24		4	3	9		50
b12	7	5	35		4	4	12		54
b12	7	6	42		5	4	12		70
b12	4	2	8		2	2	4		16
b12	4	2	8	0.01	2	4	8	0.41	28
b12	5	1	5		1	5	5		30
b12	9	6	54		6	4	12		332
b12	6	4	24		4	6	15		60
b12	7	2	14		2	7	14		62
newbyte	1	5	5	< 0.01	5	1	5	< 0.01	26
newapla2	1	6	6	< 0.01	6	1	6	< 0.01	32
c17	3	3	9	< 0.01	2	3	6	< 0.01	16
c17	4	2	8		2	2	4		18
mp2d	11	1	11		1	11	11		46
mp2d	8	6	48		5	8	20		82
mp2d	10	5	50		4	10	24		102
mp2d	6	10	60	0.01	9	3	15	0.61	318
mp2d	1	5	5		5	1	5		26
mp2d	3	6	18		5	2	8		46
mp2d	1	8	8		8	1	8		36
mp2d	5	1	5		1	5	5		28

TABLE 2: Proposed lattice sizes, lower bounds on the lattice sizes, and CMOS transistor counts for standard benchmark circuits. Each row lists the numbers for a separate output function of the benchmark circuit.

- [2] C. E. Shannon, "A symbolic analysis of relay and switching circuits," *Transactions of the AIEE*, vol. 57, no. 12, pp. 713–723, 1938.
- [3] M. L. Fredman and L. Khachiyan, "On the complexity of dualization of monotone disjunctive normal forms," *Journal of Algorithms*, vol. 21, no. 3, pp. 618–628, 1996.
- [4] T. Ibaraki and T. Kameda, "A theory of coteries: Mutual exclusion in distributed systems," *IEEE Transactions on Parallel and Distributed Systems*, vol. 4, no. 7, pp. 779–794, 1993.
- [5] S. B. Akers, "A rectangular logic array," *IEEE Transactions on Computers*, vol. 21, no. 8, pp. 848–857, 1972.
- [6] M. Chrzanowska-Jeske, Y. Xu, and M. Perkowski, "Logic synthesis for a regular layout," *VLSI Design*, vol. 10, no. 1, pp. 35–55, 1999.
- [7] M. Chrzanowska-Jeske and A. Mishchenko, "Synthesis for regularity using decision diagrams," in *Proceedings of IEEE International Symposium on Circuits and Systems ISCAS*, 2005, pp. 4721–4724.
- [8] M. M. Ziegler and M. R. Stan, "CMOS/nano co-design for crossbar-based molecular electronic systems," *IEEE Transactions on Nanotechnology*, vol. 2, no. 4, pp. 217–230, 2003.
- [9] Y. Zomaya, "Molecular and nanoscale computing and technology," in *Handbook of Nature-Inspired and Innovative Computing*. Springer, 2006, ch. 14, pp. 478–520.
- [10] Y. Cui and C. M. Lieber, "Functional nanoscale electronic devices assembled using silicon nanowire building blocks," *Science*, vol. 291, no. 5505, pp. 851–853, 2001.
- [11] Y. Huang, X. Duan, Y. Cui, L. J. Lauhon, K. Kim, and C. M. Lieber, "Logic gates and computation from assembled nanowire building blocks," *Science*, vol. 294, no. 5545, pp. 1313–1317, 2001.
- [12] Y. Luo, C. P. Collier, J. O. Jeppesen, K. A. Nielsen, E. Delonna, G. Ho, J. Perkins, H. Tseng, T. Yamamoto, J. F. Stoddart, and J. R. Heath, "Two-dimensional molecular electronics circuits," *ChemPhysChem*, vol. 3, no. 6, pp. 519–525, 2002.
- [13] A. DeHon, "Nanowire-based programmable architectures," *ACM Journal on Emerging Technologies in Computing Systems*, vol. 1, no. 2, pp. 109–162, 2005.
- [14] X. Duan, Y. Huang, and C. M. Lieber, "Nonvolatile memory and programmable logic from molecule-gated nanowires," *Nano Letters*, vol. 2, no. 5, pp. 87–90, 2002.
- [15] S. Kaeriyama, T. Sakamoto, H. Sunamura, M. Mizuno, H. Kawaura, T. Hasegawa, K. Terabe, T. Nakayama, and M. Aono, "A nonvolatile programmable solid-electrolyte nanometer switch," *IEEE Journal of Solid-State Circuits*, vol. 40, no. 1, pp. 168–176, 2005.
- [16] M. M. Eshaghian-Wilner, A. Khitun, S. Navab, and K. Wang, "A nano-scale reconfigurable mesh with spin waves," in *International Conference on Computing Frontiers*, 2006, pp. 5–9.
- [17] A. Khitun, M. Bao, and K. L. Wang, "Spin wave magnetic nanofabric: A new approach to spin-based logic circuitry," *IEEE Transactions on Magnetics*, vol. 44, no. 9, pp. 2141–2152, 2008.
- [18] K. McElvain, "IWLS93 benchmark set: Version 4.0, distributed as part of the IWLS93 benchmark distribution, <http://www.cbl.ncsu.edu:16080/benchmarks/lgsynth93/>," 1993.
- [19] A. Mishchenko, "ABC: A system for sequential synthesis and verification," 2007. [Online]. Available: <http://www.eecs.berkeley.edu/~alanmi/abc/>
- [20] R. K. Brayton, C. McMullen, G. D. Hachtel, and A. Sangiovanni-Vincentelli, *Logic Minimization Algorithms for VLSI Synthesis*. Kluwer Academic Publishers, 1984.
- [21] R. E. Bryant, "Boolean analysis of MOS circuits," *IEEE Transactions on Computer-Aided Design of Integrated Circuits and Systems*, vol. 6, no. 4, pp. 634–649, 1987.
- [22] I. Wegener, "Lower bounds on circuit complexity," in *The Complexity of Boolean Functions*. John Wiley & Sons, 1987, ch. 5, pp. 119–144.
- [23] R. K. Brayton, G. D. Hachtel, C. T. McMullen, and A. L. Sangiovanni-Vincentelli, "Multilevel logic synthesis," *Proceedings of the IEEE*, vol. 78, no. 2, pp. 264–300, 1990.
- [24] M. Altun, M. D. Riedel, and C. Neuhauser, "Nanoscale digital computation through percolation," in *Design Automation Conference*, 2009, pp. 615–616.
- [25] T. Eiter, K. Makino, and G. Gottlob, "Computational Aspects of Monotone Dualization: A Brief Survey," *Discrete Applied Mathematics*, vol. 156, no. 11, pp. 1952–2005, 2008.